CenterLineDet: Road Lane CenterLine Graph Detection With Vehicle-Mounted Sensors by Transformer for High-definition Map Creation

Zhenhua Xu, *Student Member, IEEE*, Yuxuan Liu, *Student Member, IEEE*,
Yuxiang Sun, *Member, IEEE*, Ming Liu, *Senior Member, IEEE*, and Lujia Wang, *Member, IEEE*

Abstract— With the rapid development of autonomous vehicles, there witnesses a booming demand for high-definition maps (HD maps) that provide reliable and robust prior information of static surroundings in autonomous driving scenarios. As one of the main high-level elements in the HD map, the road lane centerline is critical for downstream tasks, such as prediction and planning. Manually annotating lane centerline HD maps by human annotators is labor-intensive, expensive and inefficient, severely restricting the wide application and fast deployment of autonomous driving systems. Previous works seldom explore the centerline HD map mapping problem due to the complicated topology and severe overlapping issues of road centerlines. In this paper, we propose a novel method named CenterLineDet to create the lane centerline HD map automatically. Center-LineDet is trained by imitation learning and can effectively detect the graph of lane centerlines by iterations with vehicle-mounted sensors. Due to the application of the DETR-like transformer network, CenterLineDet can handle complicated graph topology, such as lane intersections. The proposed approach is evaluated on a large publicly available dataset Nuscenes, and the superiority of CenterLineDet is well demonstrated by the comparison results. This paper is accompanied by a demo video and a supplementary document that are available at `https://tonyxuqaq.github.io/projects/CenterLineDet/`.

I. INTRODUCTION

High-definition maps (HD maps) are critical to nowadays autonomous driving vehicles since they provide reliable information about static surroundings to assist the autonomous vehicle. HD maps have many layers consisting of various line-shaped road elements. Lower-level layers are composed of physically existing elements (e.g., road boundaries, road curbs, and road lanelines), while high-level layers have virtual elements (e.g., road lane centerlines). All of the aforementioned HD map layers are recorded in vector data format (i.e., as graphs with vertices and edges). Road elements in low-level layers of the HD map are usually utilized to prevent potential collisions and assure

Zhenhua Xu and Yuxuan Liu are with The Hong Kong University of Science and Technology (email: {zxubg,yliuhb}@connect.ust.hk).

Yuxiang Sun is with the Department of Mechanical Engineering, The Hong Kong Polytechnic University, Hung Hom, Kowloon, Hong Kong (e-mail: yx.sun@polyu.edu.hk, sun.yuxiang@outlook.com).

Ming Liu is with The Hong Kong University of Science and Technology (Guangzhou), Nansha, Guangzhou, 511400, Guangdong, China, and also with The Hong Kong University of Science and Technology, Hong Kong SAR, China, and also with HKUST Shenzhen-Hong Kong Collaborative Innovation Research Institute, Futian, Shenzhen. (email: eelium@ust.hk)

Lujia Wang is with The Hong Kong University of Science and Technology, and also with Clear Water Bay Insitute of Autonomous Driving (Shenzhen) (email: eewang@ust.hk).

Corresponding author: Lujia Wang.

the safety of vehicles. High-level layers of HD maps define the path that vehicles can drive on and contain all the topology information of roads, thus they are important for downstream tasks, such as vehicle planning, prediction and control [1]–[3]. At this stage, creating the HD map of a target region heavily relies on human annotators, which is labor-intensive, inefficient, and expensive. Therefore, an approach that automatically creates the HD map of road lane centerlines is of great interest to the industrial and research communities. Unlike low-level road elements, road lane centerlines have complicated topology structures (e.g., intersections) and severe overlapping issues, thus making the detection of lane centerline graphs challenging.

To the best of our knowledge, with multi-frame data sequence collected by vehicle-mounted sensors as input, most previous works only focus on the detection task in a single frame and output rasterized results [4]–[9], which does not meet the requirement of the HD map mapping task that demands global vectorized detection results.

Even though some previous works seek to detect road elements for vectorized map creation purposes, such as road network graph detection [10], [11], road laneline graph detection [12], [13] and road boundary detection [14]–[17], they rely on bird-eye-view (BEV) aerial images captured by satellites or UAVs, instead of data collected by vehicle-mounted sensors that we discuss in this work.

To conquer the aforementioned problems of previous works, in this paper, we present CenterLineDet (i.e., Lane CenterLine Graph Detector), a DETR-like [18] model that detects the global lane centerline graph with vehicle-mounted sensors for multi-frame and long-term HD map mapping purpose. CenterLineDet first fuses data collected by sensors in multiple frames and projects it to the BEV, then iteratively generates the global HD map by a trained DETR-like decision-making transformer network. CenterLineDet works on sequential data and does not require pre-built point cloud maps like some past works [13], [15].

The contributions of this work are as follows:

1) We present CenterLineDet, an effective deep learning approach that automatically creates the global HD map of lane centerlines with sequential data captured by vehicle-mounted sensors as input.
2) We evaluate CenterLineDet on a large publicly available dataset NuScenes [19] to demonstrate the superiority of our approach.
3) We will open source the code and data of this work.

II. RELATED WORKS

A. Applications of Road Lane Centerline HD map

Road lane centerlines are virtual lines defined by humans based on road topology, road connectivity, and traffic rules. Thus, lane centerlines contain abundant information of roads, which makes it critical for plenty of downstream tasks of autonomous vehicles, such as motion prediction [1]–[3], [20], and vehicle navigation (i.e., planning and control) [21]. Christensen *et al.* proposed an autonomous driving system for micro-mobility. The global planner and local planner of this system heavily relied on the lane centerline HD map. For the global planner, the centerline HD map was used to calculate the shortest path to the destination since it contained all the topology and connectivity information of the road network. For the local planner and controller, the vehicle was controlled to follow the lane centerline ahead (the centerline HD map defines the path that vehicles can drive on). Liang *et al.* [2] extracted features of lane centerline HD maps by a graph neural network as prior information to assist the motion prediction of objects on the road.

B. Road Element Detection with Vehicle-mounted Sensors

Most previous works resort to end-to-end perspective transformation to detect road elements in BEV [4]–[9]. In these works, with data collected by vehicle-mounted sensors as input, a deep learning network was trained to fuse the data and outputted the probabilistic distribution of target elements in the BEV. Li *et al.* [4] fused six vehicle-mounted cameras together with a LiDAR, and trained an end-to-end deep neural network to predict the BEV segmentation map of road lanelines. Based on the segmentation results of the BEV image, the authors vectorized the segmented lanelines by the skeletonization algorithm to obtain the final road laneline graph. Can *et al.* [8], [9] modeled the lane centerline by B-splies, and predicted splines in the current frame by a DETR-like network.

To the best of our knowledge, most aforementioned works only focus on the detection task in a single frame [4], [8], [9], leaving the problem of merging local maps of multiple frames into a single global map (i.e., long-term mapping problem) unexplored. Moreover, their task is the detection of simple road elements without complicated topology changes or overlapping issues, such as road boundaries and road lanelines [22]. To further improve the detection results of road elements, some works resort to additional data like Open Street Map (OSM) [21], [23] for enhancement. However, all the above works cannot well handle the following problems of lane centerline HD map mapping: (1) how to handle complicated topology and overlapping issues, especially within the road intersection areas; (2) how to merge detection results of each frame into the final global vectorized HD map.

III. METHODOLOGY

A. Overview

In this work, we aim to detect the road lane centerline graph for HD map automatic creation by using sequential vehicle-mounted sensor data. The input data of our system is a sequence of RGB images captured by six cameras (i.e, $I = \{I_i\}_{i=1}^{6}$) and point clouds obtained by a LiDAR (i.e., P). There are multiple frames in the data sequence, and T denotes the current frame. The expected output is the global graph of road lane centerlines in the world coordinate system (i.e.,$G = (V, E)$), where V is a set of lane centerline vertices, and E represents lane centerline edges connecting corresponding adjacent vertices. The approach overview is visualized in Fig. 1.

CenterLineDet has two major steps: In the current frame T, (1) predict the BEV heatmap of lane centerlines $\mathcal{H}_L$ by perspective transformation, and (2) obtain the lane centerline graph in the world coordinate system. After processing all frames in the input sequence, the expected road lane centerline graph is obtained. For the first step, we propose FusionNet which enhances the original HDMapNet [4] by combining the fully-connected neural view transformer with inverse perspective mapping (IPM), which can extract the lane centerline with better geometric accuracy. Besides $\mathcal{H}_L$, we also predict a feature tensor $\mathbf{F_T}$ and the heatmap of candidate initial vertices $\mathcal{H}_I$ by FusionNet. To conquer the prediction inconsistency of frames, we fuse the feature tensors of neighboring frames by warping and averaging.

For the second step, we propose a DETR-like transformer as the decision-making network to control an agent to generate the lane centerline graph vertex by vertex. To start up the iteration, we use local peaks in $\mathcal{H}_I$ and endpoints in the previous frame $T - 1$ as candidate initial vertices of the current frame T, which is denoted by $\mathbb{S} = \{s_k\}_{k=1}^{K}$. Vertex v_t is used to denote the current position of the agent. After concatenating the interpolated BEV feature tensor $\mathbf{F}$ with the ego historical map $\mathcal{M}_E$, an ROI $\mathbf{R}$ is cropped centering on v_t as the local visual information for the agent to make decisions. $\mathcal{M}_E$ is a binary map recording the historical trajectory of the agent in the ego vehicle coordinate system. Taken as input $\mathbf{R}$, the transformer predicts N valid vertices in the next step as a set $\mathbb{V} = \{v_{t+1}^i\}_{i=1}^{N}$. Based on N, the agent will take different actions to update the graph iteratively. When the detection of the current lane centerline instance is completed, the agent turns to another candidate initial vertex s_k and repeats the aforementioned algorithm. Once $\mathbb{S}$ is empty, we switch to process the next frame of the sequence. In the end, a graph in the world coordinate system is obtained as the predicted HD map of road lane centerlines.

More details of CenterLineDet are provided in the supplementary document.

B. Perspective Transformation

For the convenience of afterward centerline graph detection task, we convert the scene from vehicle-mounted sensors to a square BEV in advance. The BEV centers on the ego vehicle, and its x-axis aligns with the vehicle heading direction.

HDMapNet [4] applies neural view transformers to transform each perspective image feature into a local BEV feature map using fully-connected layers. Then it aligns the local
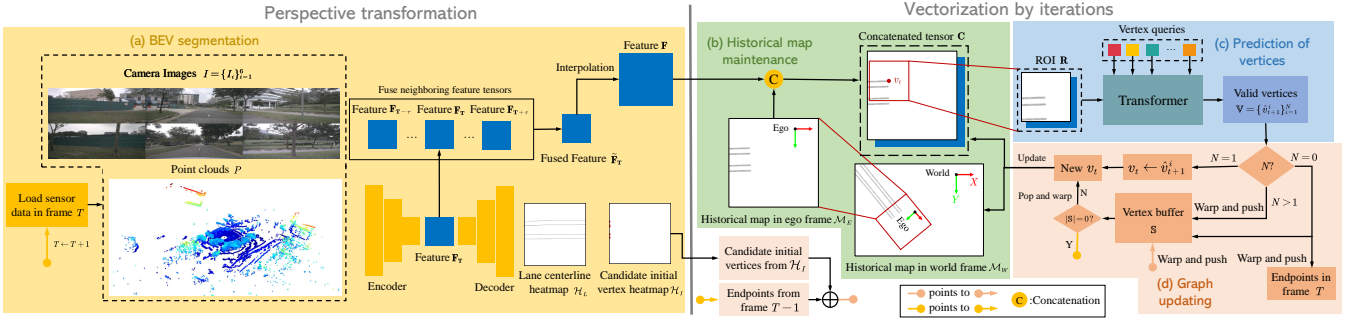
Fig. 1: CenterLineDet overview. Our proposed approach consists of two parts: perspective transformation and iterative vectorization. The first part relies on perspective transformation networks (HDMapNet/FusionNet in our work) to predict BEV heatmaps. The second part is the main contribution of this work, which trains a DETR-like transformer network to control an agent exploring the scene by iterations, whose trajectory is the global vectorized lane centerline graph.

BEV feature map with the global BEV feature map according to the extrinsic parameters of each camera. The mapping ϕ_i between the perspective view feature and the BEV feature can be denoted as:

$$\mathbf{F}_{bev}^i = \phi_i(\mathbf{F}_{I_i}), \tag{1}$$

where i is the index of the camera. In order to improve the generalization ability and the geometric precision of the feature transformation, we propose to enhance the neural view transformer with inverse perspective mapping (IPM). Based on the projective geometry of the camera, IPM computes a mapping between points in the BEV and the perspective view, and obtains a BEV feature map with solid geometric priors. The FusionNet we propose treats IPM as a shortcut without learnable parameters and ϕ_i as a learnable residual mapping function. The fused camera BEV feature map is the summation of the two mapping results:

$$\mathbf{F}_{bev} = \max_i \left\{ \mathrm{IPM}(\mathbf{F}_{I_i}) + \phi_i(\mathbf{F}_{I_i}) \right\}. \tag{2}$$

The fused BEV features are fed into a sequence of CNN networks to predict a pixel-wise lane centerline segmentation in the BEV.

C. Lane Centerline Graph Detection

In this section, we show how CenterLineDet detects the lane centerline graph and how the proposed imitation learning algorithm generates expert demonstrations to train the transformer network.

1) Inference: CenterLineDet is trained to mimic expert human annotators to create the HD map of lane centerlines vertex by vertex. It has a DETR-like transformer, a decision-making network controlling an agent to create the HD map of lane centerlines. At each step of the iteration, based on the local visual feature, the agent predicts vertices in the next step and takes corresponding actions to explore the scene. The historical trajectory of the agent is outputted as a prediction of the lane centerline graph. The inference working pipeline of CenterLineDet is shown in Fig. 1.

To record the historical information which is critical for the decision-making process of CenterLineDet, we maintain a binary historical map $\mathcal{M}_E$. Each frame has a $\mathcal{M}_E$. $\mathcal{M}_E$ is in the ego vehicle coordinate system, which is directly used to guide the decision-making of the agent, while $\mathcal{M}_W$ is in the world coordinate system to assure the consistency of $\mathcal{M}_E$ in neighboring frames.

At frame T of the input data sequence, after obtaining $\mathcal{H}_L$, $\mathcal{H}_I$ and $\mathbf{F_T}$ from the perspective transformation, we first find local peak points in $\mathcal{H}_I$ and endpoints in the previous frame as a set of candidate initial vertices $\mathbb{S} = \{s_k\}_{k=1}^K$ to initialize the iteration of CenterLineDet. Then, starting from a randomly selected s_k, CenterLineDet controls an agent to detect one lane centerline instance. Since there exists inconsistency between the BEV segmentation result of different frames, based on ego vehicle poses, we warp and project the neighboring BEV feature tensors $\mathbf{F_{T-\tau}} \sim \mathbf{F_{T+\tau}}$ to $\mathbf{F_T}$. After summation and averaging, the fused feature tensor in the current frame T is denoted as $\tilde{\mathbf{F}}_\mathbf{T}$. Then, we interpolate $\tilde{\mathbf{F}}_\mathbf{T}$ into $\mathbf{F}$, and concatenate it with $\mathcal{M}_E$. After this, an ROI $\mathbf{R}$ centering on the current vertex v_t that the agent locates is cropped, which contains sufficient visual information for the transformer to make the decision. Taken as input $\mathbf{R}$, the transformer network outputs the coordinates and valid probability of $\hat{N}$ vertices in the next step $\mathbb{V} = \{v_{t+1}^i\}_{i=1}^{\hat{N}}$. Predicted vertex v_{t+1}^i with high enough valid probability is accepted as a new vertex to update the graph. $\hat{N}$ is the same as the number of input vertex queries. Suppose we have N valid predicted vertices, then the agent should take different actions based on N to handle multiple topology structures of the lane centerline graph. $N = 0$ indicates the end of the current lane centerline in the current frame. v_t under such circumstances is treated as an endpoint, which can be a candidate initial vertex in the next frame. The agent should turn to work on another candidate initial vertex in $\mathbb{S}$. $N = 1$ means the agent moves along a lane centerline without branches, so the agent should keep moving to the next vertex v_{t+1}^i for graph updating. $N > 1$ demonstrates complicated topology structures are met, such as lane intersections, lane split, and lane merge. The agent should push all v_{t+1}^i into $\mathbb{S}$ as new candidate initial vertices, and pop one s_k from $\mathbb{S}$ to work on.
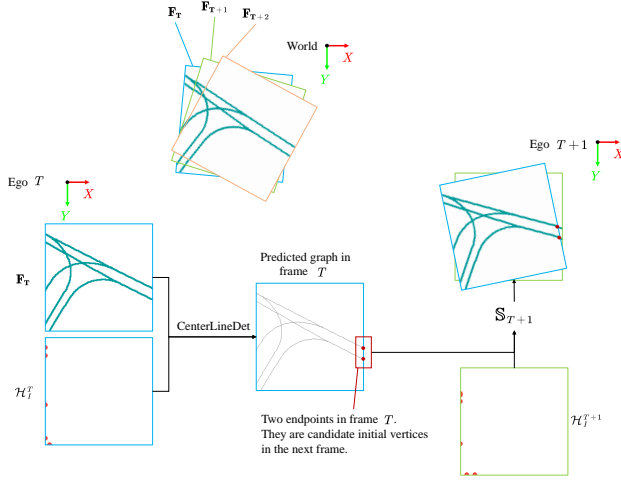
Fig. 2: Candidate initial vertices of frame $T + 1$. For better visualization, we use the ground truth lane centerline (cyan lines) to represent feature tensor **F**, which is actually a high dimension tensor in our experiments. The candidate initial vertices of frame $T + 1$ come from (1) local peaks of the heatmap $\mathcal{H}_I^{T+1}$ and (2) endpoints of frame T. Endpoints are vertices where the agent decides to stop in the previous frame. This figure is best viewed in color. Please zoom in for details.

When $\mathbb{S}$ is empty, we switch to the next frame $T+1$ of the sequence to continue the detection task. We use endpoints in the current frame (i.e.,$N = 0$) and local peaks in $\mathcal{H}_I$ of frame $T + 1$ as initialized $\mathbb{S}$ for frame $T + 1$. The candidate initial vertices in frame T is visualized in Fig. 2. For candidate initial vertices that have been explored in the past, the agent will ignore them and remove them from $\mathbb{S}$.

After all the frames of the input data sequence are processed, the trajectories of the agent is outputted as the final predicted lane centerline graph.

2) Expert demonstration sampling: In our experiments, training data is generated by a proposed sampling algorithm (i.e., expert in imitation learning). For better training efficiency, in our experiment, behavior-cloning sampling algorithm [24] is adopted. Based on breath-first-search (BFS), the sampling algorithm traversals the ground truth lane centerline graph G^* vertex by vertex. At each position v_t, it generates one training sample. To enhance the robustness of CenterLineDet, we add even distributed noise to the expert trajectory during data sampling. The simplified diagram of the sampling algorithm is visualized in Fig. 3.

During the sampling of the behavior-cloning algorithm, the ground truth label of the current step is obtained by the following equation:

$$\mathbb{V}^* = f(v_t, G^*, M_E), \tag{3}$$

where function $f(\cdot)$ can calculate the label vertices in the next step based on the ground truth graph G^* and historical information. In our experiments, $f(\cdot)$ is modified from the labeling algorithm proposed in [10], which can handle the
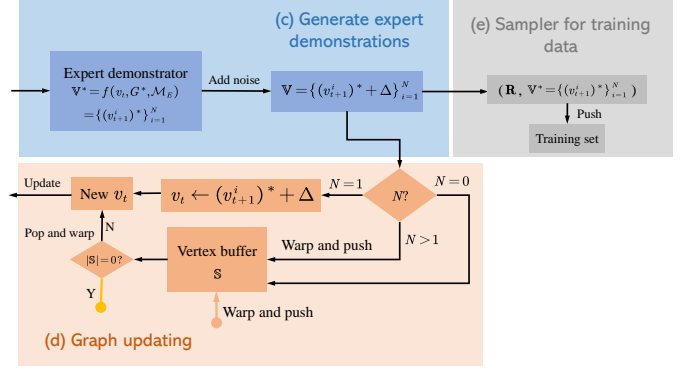

Fig. 3: Diagrams of expert demonstration sampling by behavior cloning. For simplicity, in this figure, we only visualize modules (c)-(e), while other modules of this figure are the same as that of Fig. 1.

labeling task in graphs with complicated topology. To make CenterLineDet more robust, we add random noise to $\mathbb{V}^*$ when updating the graph.

IV. EXPERIMENTAL RESULTS

To evaluate and verify the superiority of our proposed CenterLineDet, we conduct comparison experiments and ablation studies on an open sourced dataset NuScenes [19]. NuScenes is a large dataset containing data collected from various different autonomous driving scenarios. This dataset provides hundreds of data sequences collected by vehicle-mounted sensors. Each sequence has 40 frames with a 2Hz frame rate. We split around 700 sequences for training, and around 100 sequences for inference. The size of the predicted BEV is 200p×200p, corresponding to a 50m×50m-sized square region centering on the vehicle in the real world.

A. Evaluation Metrics

To evaluate the performance of approaches from both pixel-level and topology-level perspectives, we modify the metrics used in [25] for our experiments. There are three pixel-level metric scores pixel-precision (P-P), pixel-recall (P-R) and pixel-f1 (P-F) to evaluate the prediction correctness at pixel scale. Suppose we have the predicted graph $\hat{G}$ and ground truth graph G^*. For a vertex p in $\hat{G}$, if there exist one vertex q in G^* whose distance to p is smaller than a threshold δ ($\delta = 3$ pixels in our evaluations), then p is regarded as a correct prediction. Similarly, for a vertex q in G^*, if there exist one vertex p in $\hat{G}$ whose distance to q is smaller than δ, then q is correctly retrieved. The pixel-level metrics can be calculated based on the following equations:

$$
\begin{aligned}
\text{P-P} &= \frac{|\{p|\|p - q\| < \delta, p \in \hat{G}, \exists q \in G^*\}|}{|\hat{G}|} \\
\text{P-R} &= \frac{|\{q|\|p - q\| < \delta, q \in G^*, \exists p \in \hat{G}\}|}{|G^*|},
\end{aligned}
\tag{4}
$$

where $|\cdot|$ is the cardinality of a set. P-F is a combination of P-P and P-R, which is equal to $\frac{2\text{P-P}\cdot\text{P-R}}{\text{P-P}+\text{P-R}}$.

TABLE I: The quantitative results for comparison experiments.

| | Single-frame | | | | | | Multi-frame | | | | | |
| | Pixel-level ↑ | | | Topology-level ↑ | | | Pixel-level ↑ | | | Topology-level ↑ | | |
Approaches	P-P	P-R	P-F	T-P	T-R	T-F	P-P	P-R	P-F	T-P	T-R	T-F
HDMapNet [4]	0.764	0.699	0.723	0.589	0.477	0.510	0.727	0.721	0.721	0.571	0.472	0.510
TopoRoad [9]	0.408	0.566	0.461	0.501	0.397	0.443	0.410	0.526	0.477	0.357	0.406	0.380
FusionNet	0.776	0.703	0.731	0.588	0.476	0.508	0.754	**0.723**	0.735	0.569	0.470	0.507
CenterLineDet												
+HDMapNet	0.785	**0.704**	**0.733**	0.656	**0.535**	0.561	0.778	0.715	0.739	0.645	0.507	0.554
+FusionNet	**0.792**	0.697	0.730	**0.659**	0.528	**0.565**	**0.781**	0.717	**0.743**	**0.647**	**0.509**	**0.558**

There are also three metric scores to evaluate the topology correctness of the predicted graph, i.e., topology-precision (T-P), topology-recall (T-R) and topology-f1 (T-F). For each vertex q in G^*, we find all vertices in G^* that q can reach within distance ϵ as a sub-graph G_q^*. Then, we find the vertex $\tilde{p}$ in $\hat{G}$ that is closest to q and use sub-graph $\hat{G}_{\tilde{p}}$ to represent all vertices in $\hat{G}$ that $\tilde{p}$ can reach whose distance to $\tilde{p}$ is smaller than ϵ. After calculating pixel-level scores between obtained sub-graphs G_q^* and $\hat{G}_{\tilde{p}}$, we have the topology-scores:

$$\text{T-X} = \frac{\sum_{q \in G^*} \text{P-X}(G_q^*, \hat{G}_{\tilde{p}})}{|G^*|}, \tag{5}$$

where $\tilde{p}$ is the closest point in $\hat{G}$ to q, and letter X can be P, R or F.

B. Comparative Results

In this section, we evaluate CenterLineDet under different settings and baseline models to justify the superiority of our proposed approach. For a fair and comprehensive comparison, we evaluate all approaches in both single-frame and multi-frame detection tasks. Single-frame and multi-frame evaluation results are shown in Tab. I. Example results are visualized in Fig. 4.

Baselines To the best of our knowledge, very few past works have exactly the same research scope as ours, i.e., detecting the graph of road lane centerlines in sequential data collected by vehicle-mounted sensors. They either only focus on single-frame detection tasks or resort to other format input data (e.g., aerial image and OSM). Therefore, in the comparison experiments, we create our own baseline models based on past works. The evaluated approaches are listed below:

- HDMapNet [4] (ICRA2022): HDMapNet is one of the state-of-the-art approaches for road element perception and vectorization with perspective transformation, but it is mainly for single-frame detection tasks. To adapt it to our multi-frame detection task, we apply the frame merging method proposed in [22] to construct the world-level graph of lane centerlines.
- TopoRoad [9] (CVPR2022): TopoRoad is a DETR-like model, which can predict lane centerlines as B-splines in a single frame. We apply the same frame merging method as the HDMapNet baseline to merge multiple frames in the data sequence.

TABLE II: The quantitative results for multi-frame ablation studies.

| Approaches | Pixel-level ↑ | | | Topology-level ↑ | | |
	P-P	P-R	P-F	T-P	T-R	T-F
CenterLineDet-No LiDAR	0.695	0.683	0.691	0.512	0.410	0.464
CenterLineDet-No Camera	0.632	0.359	0.442	0.457	0.369	0.402
CenterLineDet	**0.781**	**0.717**	**0.743**	**0.647**	**0.509**	**0.558**

- FusionNet: FusionNet enhances HDMapNet by combining IPM with fully-connected neural view transformers to better learn the geometric transformation. Similar to HDMapNet baseline, we first obtain single-frame heatmaps and then merge them into the final multi-frame detection result.

CenterLineDet We evaluate and show the results of CenterLineDet with different perspective transformation networks (i.e., HDMapNet and FusionNet). CenterLineDet is first trained by behavior-cloning and then trained by DAgger.

Discussion From the results in Tab. I, we observe that FusionNet gains enhancement than past works, which proves the effectiveness of the fusion of IPM and fully-connected neural view transformers. For each perspective transformation model, corresponding CenterLineDet presents superior final performance, especially in multi-frame evaluations. This is because the agent controlled by CenterLineDet can make more appropriate decisions for graph detection. From visualizations in Fig. 4e, it is observed that CenterLineDet is the only approach that can distinguish centerline instances, while baselines mess up instances that causes incorrect topology.

C. Ablation Studies

In this section, we verify the importance of some modules of CenterLineDet, including the input LiDAR point clouds, input camera images and the DAgger-based sampling algorithm. The quantitative results of ablation studies are shown in Tab. II.

For LiDAR and cameras, we test the necessity of them by removing one of these sensors at a time. From Tab. II, we can see that removing either LiDAR or cameras will degrade the final results, and CenterLineDet without cameras has much inferior performance. This indicates the importance

(a) GT   (b) HDMapNet [4]   (c) TopoRoad [9]   (d) FusionNet   (e) CenterLineDet
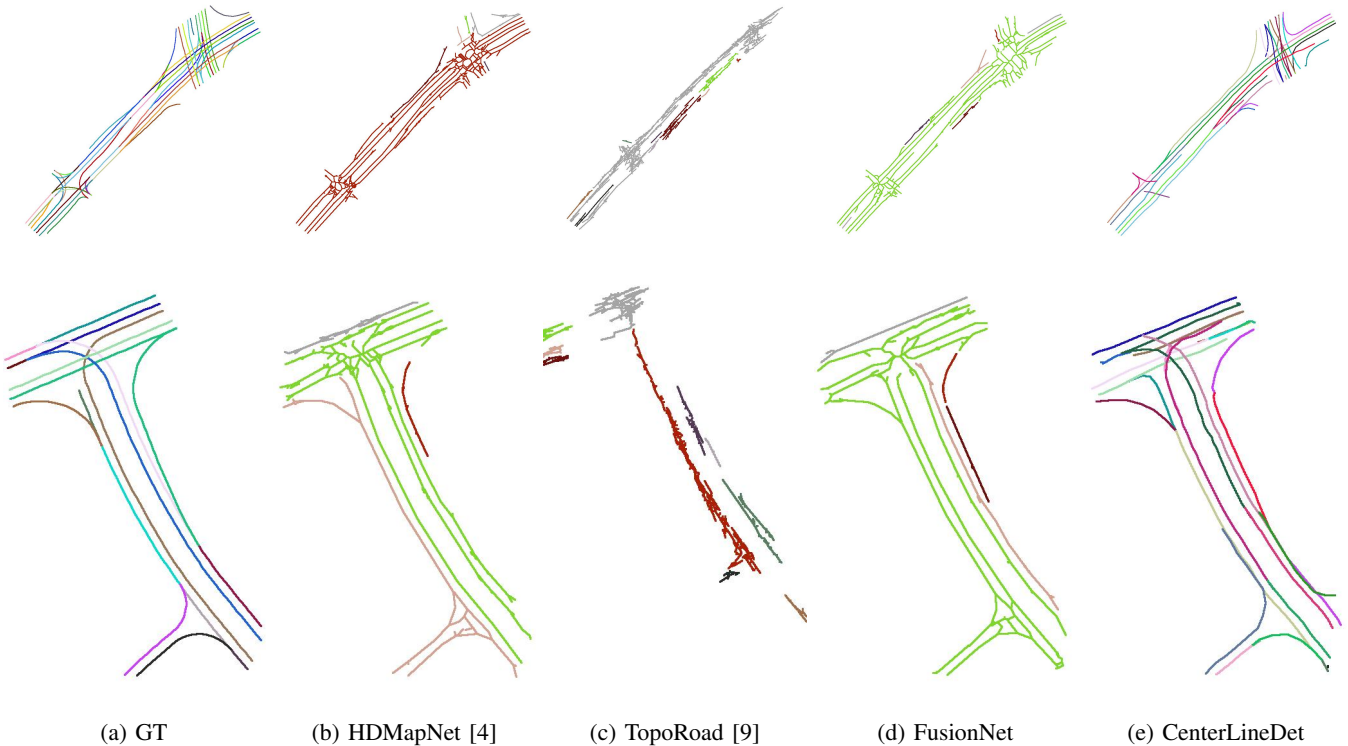
Fig. 4: Qualitative visualizations. Different colors represent different road centerline instances. CenterLineDet is the only approach that can detect and distinguish multiple instances. All baselines mess up different instances, which leads to incorrect topology, especially in the intersection area. For better visualization, graphs are widened but they are actually of one-pixel width. Please refer to the supplementary document for additional visualizations. Please zoom in for details

of data fusion, and camera images are the dominant information source of CenterLineDet. Based on the aforementioned observations, the rationality of our system design is justified.

D. Time Complexity

Our experiments were conducted on a server with a i7-8700K CPU and 4 RTX-3090 GPUs. We report experiment time usage with 4 gpus as follows:

1) It takes around 1 day to train HDMapNet or FusionNet.
2) It takes 8 minutes to inference 4000 frames (100 scenes) for HDMapNet or FusionNet.
3) It takes 4 hours for behavior cloning sampling, and it takes 1 extra day to train CenterLineDet with behavior-cloning sampled data.
4) It takes overall 28 minutes for CenterLineDet to inference 4000 frames (0.42s/frame=2.39Hz, which is sufficient for Nuscenes with 2Hz key frame rate). Besides, it should be noted that CenterLineDet does not need to work in an online manner (i.e., HD map mapping task is not an online task), thus even a lower frame rate should also be sufficient.

E. Limitation

This paper claims two limitations of the proposed approach: (1) CenterLineDet is restricted the perspective transformation performance. CenterLineDet is of two stages and cannot be trained in an end-to-end manner, which degrades the final performance. If the perspective transformation module presents awful BEV heatmaps, CenterLineDet would be greatly affected. (2) Although CenterLineDet presents the best performance in evaluation experiments, it still cannot handle very complicated intersection areas. We aim to solve this problem by applying more powerful perspective transformation models.

V. CONCLUSION AND OUTLOOK

We presented CenterLineDet in this paper for the automatic creation of the lane centerline HD map by vehicle-mounted sensors. The key problem was detecting the lane centerline graph with complicated topology. Taken as input data sequences from multiple sensors, CenterLineDet first predicted the BEV segmentation heatmap of lane centerlines. Then, a decision-making transformer network was trained to control an agent exploring the scene to create the lane centerline graph vertex by vertex. After processing all frames of the input data sequence, the trajectory of the agent was outputted as the lane centerline graph for HD map creation. The effectiveness and superiority of CenterLineDet were demonstrated by the comparison experiments on a publicly available dataset. In the future, we plan to adopt more powerful perspective transformation models and make CenterLineDet end-to-end trainable.

References

[1] J. Gao, C. Sun, H. Zhao, Y. Shen, D. Anguelov, C. Li, and C. Schmid, "Vectornet: Encoding hd maps and agent dynamics from vectorized representation," in *Proceedings of the IEEE/CVF Conference on Computer Vision and Pattern Recognition*, 2020, pp. 11 525–11 533.

[2] M. Liang, B. Yang, R. Hu, Y. Chen, R. Liao, S. Feng, and R. Urtasun, "Learning lane graph representations for motion forecasting," in *European Conference on Computer Vision*. Springer, 2020, pp. 541–556.

[3] F. Da and Y. Zhang, "Path-aware graph attention for hd maps in motion prediction," *arXiv preprint arXiv:2202.13772*, 2022.

[4] Q. Li, Y. Wang, Y. Wang, and H. Zhao, "Hdmapnet: A local semantic map learning and evaluation framework," 2021.

[5] B. Pan, J. Sun, H. Y. T. Leung, A. Andonian, and B. Zhou, "Cross-view semantic segmentation for sensing surroundings," *IEEE Robotics and Automation Letters*, vol. 5, no. 3, pp. 4867–4873, 2020.

[6] B. Zhou and P. Krähenbühl, "Cross-view transformers for real-time map-view semantic segmentation," *arXiv preprint arXiv:2205.02833*, 2022.

[7] J. Philion and S. Fidler, "Lift, splat, shoot: Encoding images from arbitrary camera rigs by implicitly unprojecting to 3d," in *European Conference on Computer Vision*. Springer, 2020, pp. 194–210.

[8] Y. B. Can, A. Liniger, D. P. Paudel, and L. Van Gool, "Structured bird's-eye-view traffic scene understanding from onboard images," in *Proceedings of the IEEE/CVF International Conference on Computer Vision*, 2021, pp. 15 661–15 670.

[9] ——, "Topology preserving local road network estimation from single onboard camera image," *arXiv preprint arXiv:2112.10155*, 2021.

[10] Z. Xu, Y. Liu, L. Gan, Y. Sun, M. Liu, and L. Wang, "Rngdet: Road network graph detection by transformer in aerial images," *arXiv preprint arXiv:2202.07824*, 2022.

[11] F. Bastani, S. He, S. Abbar, M. Alizadeh, H. Balakrishnan, S. Chawla, S. Madden, and D. DeWitt, "Roadtracer: Automatic extraction of road networks from aerial images," in *Proceedings of the IEEE Conference on Computer Vision and Pattern Recognition*, 2018, pp. 4720–4728.

[12] N. Homayounfar, W.-C. Ma, S. Kowshika Lakshmikanth, and R. Urtasun, "Hierarchical recurrent attention networks for structured online maps," in *Proceedings of the IEEE Conference on Computer Vision and Pattern Recognition*, 2018, pp. 3417–3426.

[13] N. Homayounfar, W.-C. Ma, J. Liang, X. Wu, J. Fan, and R. Urtasun, "Dagmapper: Learning to map by discovering lane topology," in *Proceedings of the IEEE International Conference on Computer Vision*, 2019, pp. 2911–2920.

[14] Z. Xu, Y. Sun, and M. Liu, "Topo-boundary: A benchmark dataset on topological road-boundary detection using aerial images for autonomous driving," *IEEE Robotics and Automation Letters*, vol. 6, no. 4, pp. 7248–7255, 2021.

[15] J. Liang, N. Homayounfar, W.-C. Ma, S. Wang, and R. Urtasun, "Convolutional recurrent network for road boundary extraction," in *Proceedings of the IEEE Conference on Computer Vision and Pattern Recognition*, 2019, pp. 9512–9521.

[16] Z. Xu, Y. Liu, L. Gan, X. Hu, Y. Sun, L. Wang, and M. Liu, "csboundary: City-scale road-boundary detection in aerial images for high-definition maps," *arXiv preprint arXiv:2111.06020*, 2021.

[17] Z. Xu, Y. Sun, and M. Liu, "icurb: Imitation learning-based detection of road curbs using aerial images for autonomous driving," *IEEE Robotics and Automation Letters*, vol. 6, no. 2, pp. 1097–1104, 2021.

[18] N. Carion, F. Massa, G. Synnaeve, N. Usunier, A. Kirillov, and S. Zagoruyko, "End-to-end object detection with transformers," in *European Conference on Computer Vision*. Springer, 2020, pp. 213–229.

[19] H. Caesar, V. Bankiti, A. H. Lang, S. Vora, V. E. Liong, Q. Xu, A. Krishnan, Y. Pan, G. Baldan, and O. Beijbom, "nuscenes: A multimodal dataset for autonomous driving," in *Proceedings of the IEEE/CVF conference on computer vision and pattern recognition*, 2020, pp. 11 621–11 631.

[20] T. Liu, Q. hai Liao, L. Gan, F. Ma, J. Cheng, X. Xie, Z. Wang, Y. Chen, Y. Zhu, S. Zhang *et al.*, "The role of the hercules autonomous vehicle during the covid-19 pandemic: An autonomous logistic vehicle for contactless goods transportation," *IEEE Robotics & Automation Magazine*, vol. 28, no. 1, pp. 48–58, 2021.

[21] Y. Zhou, Y. Takeda, M. Tomizuka, and W. Zhan, "Automatic construction of lane-level hd maps for urban scenes," in *2021 IEEE/RSJ International Conference on Intelligent Robots and Systems (IROS)*. IEEE, 2021, pp. 6649–6656.

[22] M. Elhousni, Y. Lyu, Z. Zhang, and X. Huang, "Automatic building and labeling of hd maps with deep learning," in *Proceedings of the AAAI Conference on Artificial Intelligence*, vol. 34, no. 08, 2020, pp. 13 255–13 260.

[23] A. Joshi and M. R. James, "Generation of accurate lane-level maps from coarse prior maps and lidar," *IEEE Intelligent Transportation Systems Magazine*, vol. 7, no. 1, pp. 19–29, 2015.

[24] T. Osa, J. Pajarinen, G. Neumann, J. A. Bagnell, P. Abbeel, and J. Peters, "An algorithmic perspective on imitation learning," *arXiv preprint arXiv:1811.06711*, 2018.

[25] S. He and H. Balakrishnan, "Lane-level street map extraction from aerial imagery," in *Proceedings of the IEEE/CVF Winter Conference on Applications of Computer Vision*, 2022, pp. 2080–2089.